ELM control at the L → H transition by means of pellet pacing in the ASDEX Upgrade and JET all-metal-wall tokamaks

P. T. Lang, H. Meyer[1], G. Birkenmeier, A. Burckhart, I. S. Carvalho[2], E. Delabie[3], L. Frassinetti[4], G. Huijsmans[5], G. Kocsis[6], A. Loarte[5], C.F. Maggi, M. Maraschek, B. Ploeckl, F. Rimini[1], F. Ryter, S. Saarelma[2], T. Szepesi[6], E. Wolfrum, ASDEX Upgrade Team and JET Contributors*

MPI für Plasmaphysik, Boltzmannstr. 2, 85748 Garching, Germany
JET-EFDA, Culham Science Centre, Abingdon, OX14 3DB, UK
1) Culham Centre for Fusion Energy, Culham Science Centre, Oxfordshire, OX14 3DB, UK
2) Instituto de Plasmas e Fusão Nuclear, Instituto Superior Técnico, Universidade de Lisboa, P-1049-001 Lisboa, Portugal
3) FOM-DIFFER, NL-3430 BE Nieuwegein, The Netherlands
4) Royal Institute of Technology (KTH), Valhallavägen 79, 100 44 Stockholm, Sweden
5) ITER Organization, Cadarache, F-13067 Saint-Paul-lez-Durance, France
6) Wigner RCP, RMI, Konkoly Thege 29-33, H-1121 Budapest, Hungary
*See Appendix of Romanelli F. et al., 2012 Proceedings of the 24th IAEA Fusion Energy Conference, San Diego, USA

ABSTRACT

In ITER pellets are envisaged for ELM control and fuelling. More important, ELM control, particularly control of the first ELM needs to be demonstrated already in the non-nuclear phase of ITER during operation in H or He. Whilst D pellets have been established as ELM control technique in the stationary phase with D target plasmas in devices with C as plasma-facing component, the question of other isotopes and non-stationary phases are not so well known. Here, we report on new pellet triggering experiments in ASDEX Upgrade and JET mimicking specific ITER operating scenarios. Both machines are equipped with an all-metal wall, where recent investigations have shown that pellet triggering and pacing become more intricate. In both machines ELM triggering by D pellets injected into D plasmas during extended ELM-free phases, often following the L → H transition, has been demonstrated. In both devices the pellets are found to induce ELMs under conditions far from the stability boundary for type-I ELMs. Near the L → H transition, induced ELMs in some cases might more likely have type-III rather than type-I characteristics. Furthermore, in ASDEX Upgrade this study was conducted during L → H transitions in the current ramp-up phase as envisaged for ITER. In addition, the pellet ELM trigger potential was proven in ASDEX Upgrade with a correct isotopic compilation for the non-nuclear phase in ITER, viz. H pellets into either He or H plasmas.
Results from this study are encouraging since they have demonstrated the pellets' potential to provoke ELMs even under conditions quite far from the stability boundaries attributed to the occurrence of spontaneous ELMs. However, with the recent change from carbon to an all-metal plasma-facing components examples have been found in both machines where pellets failed to establish ELM control under conditions where this would be expected and needed. Consequently, a major task of future investigations in this field will be to shed more light on the underlying physics of the pellet ELM triggering process to allow sound predictions for ITER.

Keywords: ELM control, tokamak, pellet

INTRODUCTION

Operating ITER in the reference inductive scenario at the design values I_P = 15 MA and Q_{DT} = 10 relies on good H-mode confinement facilitated by the presence of a strong edge transport barrier and a sufficiently high plasma pressure pedestal. The steep gradients evolving at the edge can drive MHD instabilities resulting in an Edge-Localized Mode (ELM) producing a rapid energy burst from the pedestal region. Without dedicated ELM control, the resulting transient heat loads on plasma-facing materials in ITER become critical for operation at a plasma current $I_P \approx 9.5$ MA [1]; progressing to a higher I_P would result in an intolerably short lifetime of the divertor plates [2]. Currently, several options are being considered for this inevitable ELM actuation, but all of them need further validation for the ITER tasks. Obviously, the main task in this context is to achieve sufficient mitigation of the peak power flux to the divertor in appropriate scenarios, either by suppression or mitigation of ELMs. Attention has recently been focussed on ELM control requirements in ITER [1] in relation to the proposal to start ITER operation with a tungsten (W) divertor, which was originally envisaged for the beginning of nuclear operations (DD and DT plasmas) and is now being planned also for the start of ITER operation in the non-nuclear phase (H and He plasmas) [3].

For initial ITER operation the plasma current will be limited to $I_P \approx 7.5$ MA, and hence ELMs are not likely to cause unacceptable divertor erosion or melting. However, W will be produced in between and by the ELMs. Hence, a minimum ELM frequency may be required to maintain a sufficiently low W concentration in the main plasma [1]. Since ITER is expected to enter the H-mode already during the current ramp-up phase, the mitigation technique must be compatible with an evolving plasma shape and edge magnetic safety factor. Hence, any control tool considered requires demonstration of successful actuation already immediately before and during the L → H transition. Crucial questions are whether the technique has an impact on the L → H transition power threshold and whether there is a residual influence on the final steady-state H-mode.

Injection of solid pellets formed from frozen fuel has been demonstrated as a very well-proven technique for control of the ELM frequency in several tokamaks, e.g. ASDEX Upgrade (AUG) [4], JET [5] and DIII-D [6,7]. Consequently, a suitable system is being developed for controlled ELM triggering in ITER by injecting pellets carrying at least 2.0 x 10^{21} particles [1] from the torus outboard [8].

Here, we report on corresponding experiments conducted at AUG and JET. Employing pellet injection for ELM control at the L → H transition, they aim to mimic initial ITER conditions (H pellets in H/He plasma during I_P ramp). Although full coverage of all aspects in a single demonstration experiment could not be achieved, all critical issues were covered one by one.

SET-UP

The experiments reported were conducted in the AUG and JET tokamaks, both operated with all-metal walls.

AUG is a medium-sized divertor tokamak (major radius R_0 = 1.65 m, minor radius a_0 = 0.5 m, I_P of up to 1.4 MA, toroidal magnetic field B_t of up to 3.1 T) with high shaping capability. It is equipped with a versatile set of auxiliary heating systems comprising 20 MW neutral beam injection (NI), up to 6 MW ion cyclotron resonance heating (ICRH) coupled power, and 5 MW electron cyclotron resonance heating (ECRH). All plasma-facing components were converted stepwise from initially carbon (C) to W; complete W coverage has now been achieved. For details see [9] and the references therein. The investigations reported here were all performed in the divertor IIc configuration, with a plasma volume of typically about 12 m^3. Particle inventories of the target plasma used in this study were of the order of 6 x 10^{20} D.

The investigations at ASDEX Upgrade used the refurbished high-speed launcher system based on a centrifuge accelerator and a looping transfer system. The system, initially developed for fuelling purposes, is capable of delivering pellets covering a wide range of size and speed at repetition rates of up to 80 Hz from the torus inboard inclined at an angle of 72^{o} with respect to the horizontal mid-plane [10]. Strong and efficient fuelling results essentially from the inboard launching scheme owing to an ExB major radius drift of the pellet cloud [11]. Notably, such large density perturbations intrinsically caused by a set up optimized for fuelling purposes is not ITER-like. In ITER, outboard injection employing pellets with a more appropriate size will avoid this caveat [1].

For operation in AUG with D ice, reliable and persistent operation is achieved for the entire parameter regime. Experiments employing H pellets were essentially performed with large pellets at low to moderate speed. Since the cryostat system is mainly designed for operation with D ice, the lower triple-point temperature of H in relation to D resulted in deficient cool-down of the H ice rod. Hence, the lower yield strength of the pellets led to reduced reliability of delivery, being in particular too low for the task of ELM control with small pellets. The pellet observation system was upgraded as well and now allows fast individual pellet tracking.

For the smallest possible pellet size the designated particle inventory is 1.5 x 10^{20} D, while large pellets contain nominally 3.7 x 10^{20} D. Although a significant fraction of the pellet mass is lost during the transfer, the amount, dependent on pellet size and speed, predominantly intended for a particle fuelling system already significantly increases the plasma density with every single pellet. A continuous pellet train as applied for ELM control purposes has an even greater impact on the plasma, causing considerable alteration of the initial plasma parameters. Hence, the magnitude of the unavoidable fuelling by the pellet in AUG is always significant.

The world's largest divertor tokamak, JET (R_0 = 2.96 m, a_0 = 1.25 m, $I_P \leq$ 4.5 MA, $B_t \leq$ 3.8 T), has been operated since 2012 with the ITER-Like Wall (ILW). This metallic wall replaced previous C plasma-facing components by a combination of beryllium (Be) in the main chamber and W in the divertor, the configuration envisaged for ITER. The design of the ILW components took into account plasma operation at high auxiliary powers of up to 40 MW (NBI 35 MW and ICRF 5 MW) for up to 20 s [12]. Pellets at JET are produced by the high-frequency pellet injector (HFPI), installed at the end of 2007 and subsequently modified several times [13]. The HFPI system was originally designed to launch pellets from three different injection sites either for fuelling or for ELM pacing purposes. The pellet speed can be adjusted by the propellant gas pressure in the blower gun acceleration unit. The size and hence pellet mass can be fine-tuned by the pellet length. In addition, two different diameters can be chosen for the extruded ice rod. While a diameter of 4 mm produces large pellets designed for core fuelling, small pellets 1.5 mm in diameter have been adapted for the specific needs of the ELM control task. In operation, it was found that reliable pellet delivery could only be achieved when large pellets were launched from the torus outboard. While the full designated repetition rate of 15 Hz was achieved for large pellets, for the small pacing-size pellets only one of the two installed extruders works reliably up to 25 Hz rather than the nominal 50 Hz for pacing. A further revision is ongoing, expected to be finished by mid-2015. The aim is to optimize the system now for reliable delivery of small pellets for pacing purposes. Therefore, two transfer lines (outboard and inboard) hampered by an unfavourable track with multiple bends were rationalized focussing efforts now entirely on the vertical inboard launch track. Economising to the single launch site providing most favourable transfer conditions and allowing for a considerable shortening and simplification of the guiding system is expected to allow for operation with full performance in respect of variability and reliability. Fortunately, recent results indicated pellets launched from the vertical inboard track can trigger ELMs also most readily.

Pacing-size pellets as applied in this study have a designated particle inventory of 2.1 x 10^{20} D. However, with a plasma volume of typically about 80 m^3 and target plasma particle inventories of the order of 24 x 10^{20} D, the fuelling impact of the pellets becomes almost marginal when pellet rates are restricted to reasonably low values.

FIRST DEMONSTRATION AT ASDEX UPGRADE

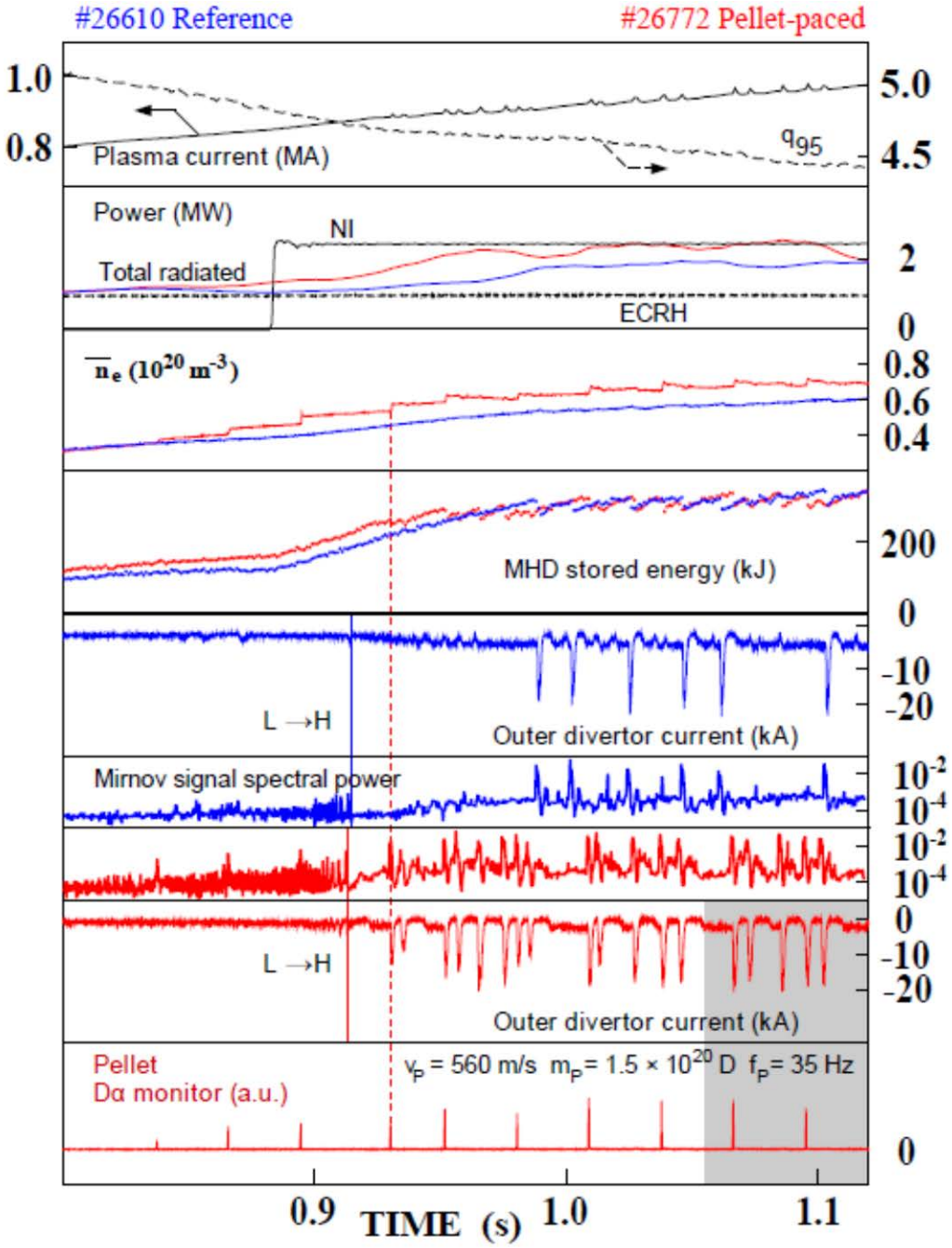

Figure 1: Demonstration of ELM control by pellet pacing at ASDEX Upgrade while the plasma undergoes the L → H transition during current ramp-up (first box). Reference discharge (#26610, blue traces) showing an ELM-free phase; discharge with pellet pacing (#26772, red traces) showing ELM activity virtually immediately after the L → H transition. Line integrated density evolution (third box) measured by laser interferometer; pellet monitoring (lowermost box) by ablation radiation measured by wide angle diode.

Pellet pacing through the L→H transition during the current ramp-up was tested on AUG initially with D pellets into a D plasma, and compared with a reference shot without pellets. During this phase the plasma shape and q_{95} still evolve. The pellet-controlled shot (#26772, red traces) is shown together with the reference discharge (#26610, blue traces) in Figure 1. Small differences during the plasma start-up phase and apparently the impact of the pellet fuelling making the plasma more resistive cause a slightly faster increase of the plasma stored MHD energy in the pellet-controlled shot. The reference discharge shows a delay of about 70 ms between entering the H-mode and the first ELM in the absence of active ELM control. ELMs are monitored by very simple and robust indirect measurement of the divertor load: the (thermo-) electric current into an outer divertor tile, measured as voltage at a shunt resistor embedded in the tile mounting [14], referred to as "Outer divertor current". Details of some spontaneous and triggered ELMs are shown in Figure 2 on an expanded time scale; the entire period displayed in Figure 2 refers to the grey-shaded area in the lower right part of Figure 1.
The L → H transition is facilitated by an early heating phase applying a single NI beam. The phase transition can be identified by the beginning of barrier formation, indicated by the corresponding evolution of the edge density and the spin-up of poloidal rotation. The transition can be recognized here also in the temporal evolution of the ELM monitor or the magnetic perturbations measured by Mirnov coils. A short phase with low turbulence, visualized here by the sudden drop in the "Mirnov signal spectral power" (coil signal integrated from 0 - 100 kHz), is observed here just after the transition. For this scenario, the threshold power for H-mode access due to the ITPA threshold scaling [15] is about 2.0 MW; however, careful investigation showed this value is reduced by about 25% in AUG since operated with an all-W wall [16]. Hence, with a loss power (absorbed heating power – dW/dt) of about 2.0 MW the plasma is still in the vicinity of the threshold. Sustained injection of pellets all through the L → H transition considerably reduced the duration of the ELM-free phase. Pellets arriving a few ms before the transition clearly do not trigger ELM-like events. Pellets reaching the plasma immediately after the transition do trigger ELMs. In particular, the first ELM is already triggered before the plasma energy approaches its final level. Several spontaneous ELMs follow the triggered ones caused by the fuelling effect of the pellets. In both discharges, the gas puff rate was kept steady at 8×10^{20} D/s. Pellet pacing thus increased the total averaged particle flux by about 60%. This resulted in approx. 40% increased divertor density and an elevated line averaged density as displayed in Figure 1; however, this did not show a significant impact on the confinement finally attained.
Pellet injection did not show a major impact on the L→ H transition or cause an almost prompt transition due to the changed edge parameters in our investigation. Such effects have been e.g. reported from, for example, DIII-D [17] and MAST, where pellet fuelling from the high-field side allows access to H-mode in plasmas heated by neutral beams [18]. However, although in both cases the L→ H transition took place at virtually the same time, the plasma energy attained in the pellet case at this time was somewhat higher.

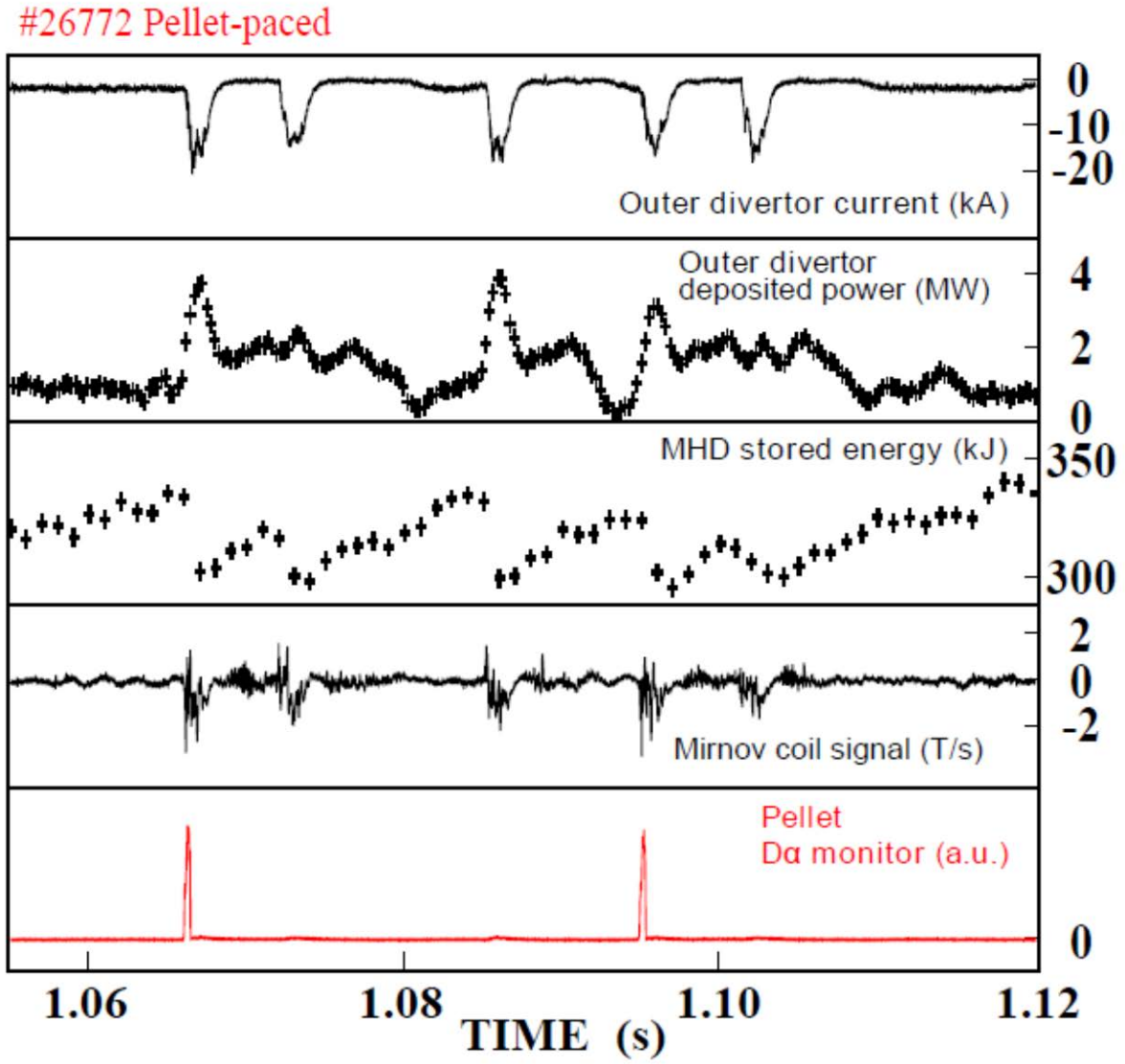

Figure 2: Details of some spontaneous and triggered ELMs; the period displayed here refers to the grey-shaded area in the lower right part of Figure 1.

ISOTOPE ADAPTION: H PELLETS IN HE AND H PLASMAS

To match the ITER requirements for the initial phase, experiments with correct isotopic compilation were conducted on AUG. The technically more challenging launch of H pellets into H and He plasmas was demonstrated as well. With the operational restrictions already mentioned, this is accompanied by a strong fuelling impact, even more pronounced than in the case shown in Figure 1.

A plasma scenario similar to that used in D (see Figure 1), but with He as the main ion species was developed, as shown in the left part of Figure 3. Again, early heating triggered a first L → H transition already during the current ramp-up, with the plasma shape still changing. However, a dithering phase evolves owing to marginal heating power [19]. A recent investigation performed at DIII-D attributes the occurrence of dithering to a predator - prey limit cycle oscillation driven by turbulent transport into L-mode and self-organized shear flow supporting barrier formation into H-mode [20]. The spectral power of the MHD activity obtained from the signal trace marked by the red box in the left part,

recorded by a pick-up coil (mounted at the torus low field side slightly below the horizontal mid plane to the inner vessel wall) is shown in the right part of Figure 3. It includes both a pellet already arriving in the L- and the dithering phase (onset of pellet ablation marked by arrows) and several spontaneous dithering events. The frequency distribution of the spectral power for the first pellet arriving in this dithering phase seemingly looks as if composed from a pure pellet component as observed for the previously injected pellet during the L-mode, and the pure dithering signature.

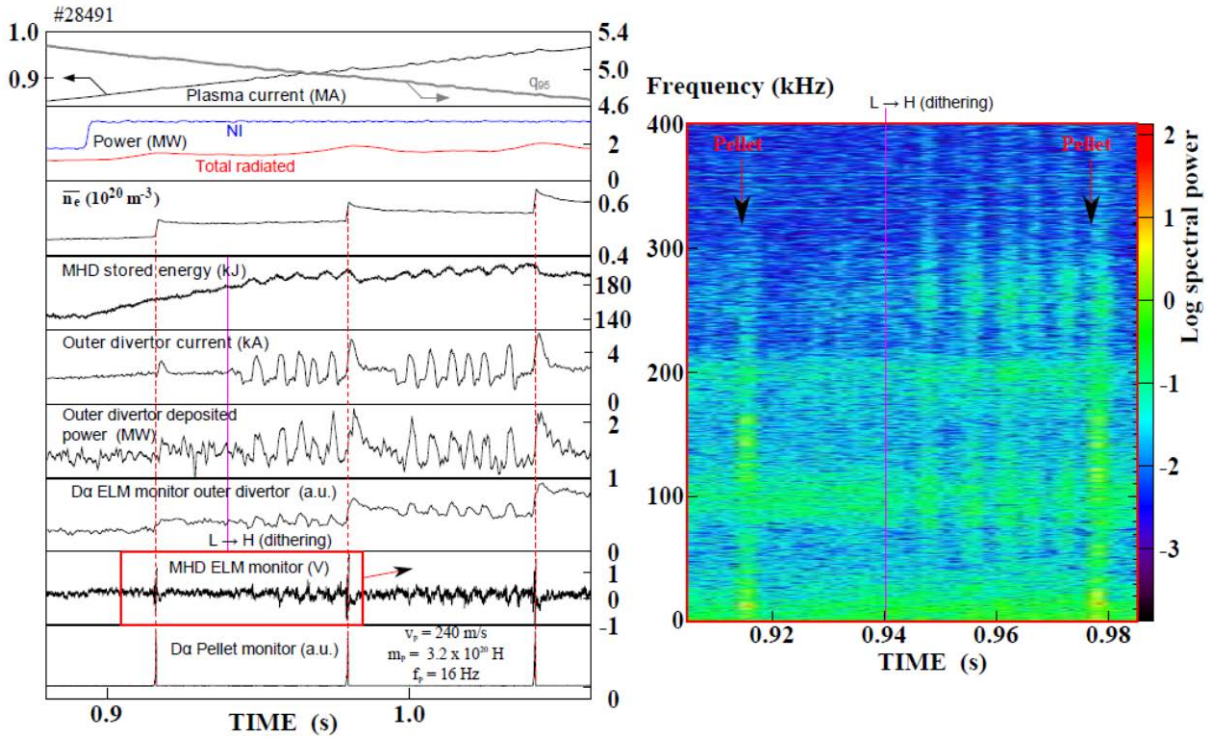

Figure 3: Left part: Pellet ELM triggering attempt at ASDEX Upgrade using H pellets injected into a He plasma. However, the first L → H transition is followed by a dithering phase; pellets (indicated by dashed lines) arrive both before and after this transition. Right part: Detailed analysis of the MHD activity signal, marked by red box in left part. Onset of pellet ablation indicated by the arrows.

The unfavourably high threshold power expected for H-mode access, makes operation with H the less probable non-nuclear start-up scenario for ITER [1]. However, with respect to pellet-based ELM controlling it could be the favourable option since no dilution of the target plasma would take place. In order to cover this scenario as well, H pellet injection into a H target plasma was tested.

To do this, a scenario with long-lasting ELM-free phase of more than 200 ms duration in the reference case was developed. The L → H transition was initiated during the plasma current flat-top phase by sudden application of pure EC wave heating into an initial ohmic phase. Pellets were injected at a very low frequency of 5 Hz to avoid too drastic a fuelling effect. Figure 4 displays the result. The left part shows the reference phase without pellets and the long ELM-free phase following the L → H transition. Once again, the outer divertor current is taken for monitoring the appearance of ELMs. The right part of Figure 4 presents data from the following shot, repeated with identical discharge setting but with pellets added (marked by the arrows) to the second last pane of the right panel. The strong fuelling impact of the pellets is clearly visible. The massive pellet perturbation outstrips some of the ELM

signatures. It seems the first pellet after the L → H transition triggers an ELM already about 130 ms after the transition; however jointly a massive perturbation is introduced altering the evolution of the discharge significantly. Spontaneous ELM activity sets in only after about 200 ms just as in the reference case. No corresponding event is triggered by the pellet arriving prior to the L → H transition.

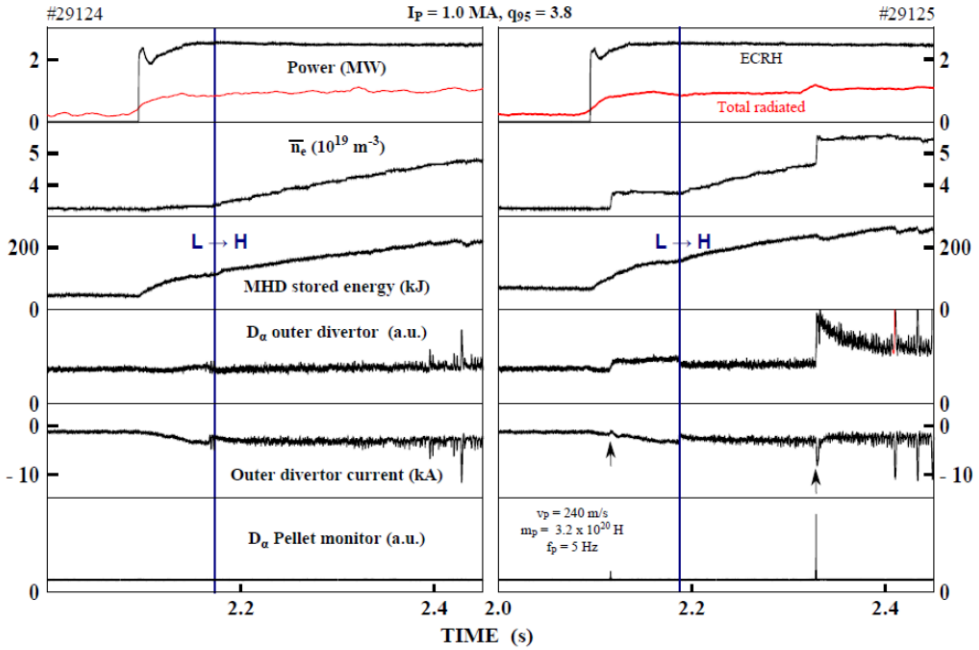

Figure 4: Demonstration of the pellet ELM trigger potential at ASDEX Upgrade for H pellets injected into a H plasma. A 200-ms-long ELM-free phase is established in the reference case (left), whereas already the first pellet arriving after the L →H transition seemingly triggers an ELM, but also causes a massive perturbation (pellet rate 5 Hz, arrival marked by arrows).

CONFIRMATION AT JET AND ELIMINATION OF THE FUELING IMPACT

Interpretation of all experiments performed at AUG is complicated by the unfavorable ratio of pellet-to-plasma particle content. Efforts to produce and launch sub-mm pellets were unproductive. The increasingly unfavourable surface/volume ratio and dwindling heat capacity of the tiny ice bodies were most probably the reason why smaller pellets showed a rapid decrease of delivery efficiency as fragmentation and dissolving sets in. Hence, fuelling inevitably caused by the pellets always results in a significant impact on plasma density in a tokamak of AUG size. This situation can clearly be improved at JET when pellets of about the same size as the smallest reliable ones at AUG are injected. The much larger plasma volume of JET now makes the total density build-up no longer perturbative.

Experiments reported here were embedded in studies of the L → H transitions investigating the power threshold dependence on the plasma shape [21]. This investigation also assessed the impact of the fuelling method and location on the threshold value. Replacing the gas puff partially by pellets (again D pellets in D plasmas) in the scenario used (I_P = 2.0 MA, B_t = 2.4, q_{95} = 3.5, elongation ε = 1.7, upper and, lower triangularity δ_u = 0.24 and δ_l = 0.18, respectively) showed that pellets do have higher fuelling efficiency but do not alter the transition parameters with respect to density and heating power [21]. The reference discharge (JPN84726, left part of Figure 5) with pure gas fuelling (applied gas puffing rate displayed in the lowermost box) shows a pronounced ELM-free phase lasting about 110 ms after the L → H transition. In this case, ELMs are monitored by the increased Be impurity radiation from

the outer divertor strike point region, caused by the ELM induced power flux; for details see [22]. Partial pellet fuelling by launching a train of pacing size at a rate of 25 Hz (JPN84730, right part of Figure 5; the averaged pellet particle flow rate is displayed together with the applied gas puffing rate) results in a slightly higher density in the L-mode phase owing to better fuelling efficiency. In the H-mode phase a fuelling efficiency similar to that in the gas reference is found. But now every pellet triggers an ELM and the resulting ELM control avoids the ELM-free phase. The moderate density rise per injected pellet resulted in a density evolution reasonably matching the gas-fuelled reference discharge.
The higher density during the L-mode phase in the pellet cased, the L → H transition to occur later than in the reference discharge, and the pre-set timed pellet monitor ran out of data memory. Hence, pellet arrival in the plasma had to be estimated from a time-of-flight analysis of the pellets passing through several cavities installed along the flight tubes, as shown in the lower box. The pellet speed scatter is appreciable, resulting in a distorted pellet train frequency. Furthermore, a gap due to a pellet obviously destroyed in flight is precisely mirrored by the ELMs.

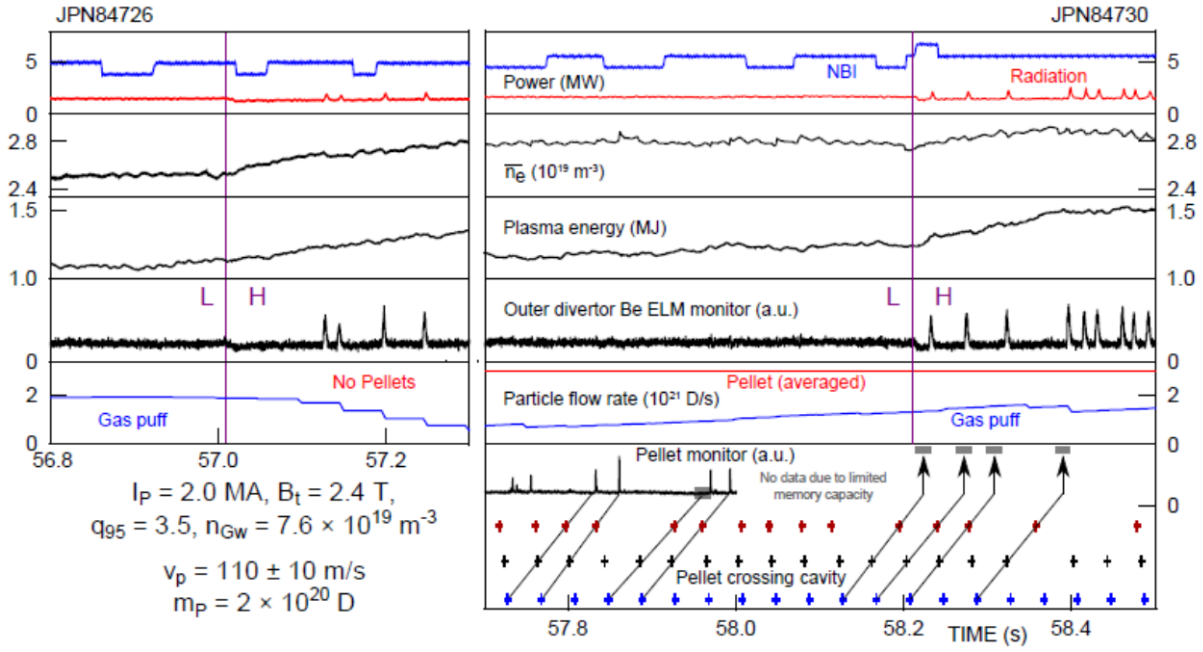

Figure 5: Demonstration of ELM control at JET by pellet pacing while the plasma undergoes the L → H transition. The reference discharge (left) shows a long ELM-free phase. This is avoided by pellet pacing (right), the first ELM being triggered shortly after the L → H transition with the plasma parameters still close to L-mode values. Pellet arrival in the plasma is estimated from a time-of-flight analysis (lower box, uncertainty represented by the grey bars).

STABILITY ANALYSIS OF THE JET DEMONSTRATION CASE

Already our investigations at AUG clearly show that ELMs can be triggered under circumstances where no spontaneous ELMs seem to occur yet. This indicates that the strong external perturbation locally created by the pellet ablation plasmoid hits the stability limit in the edge already before this happens, driven by internal plasma perturbations (e.g. fluctuations). Clearly, this calls for closer investigation of the situation. Hampered by the fact that the strong pellet fuelling impact significantly distorts the pedestal region with respect to the reference cases, the AUG experiments are obviously not especially well suited to such

detailed analysis. On the other hand, the JET experiment presented above provides good data for the stability analysis. The discharges, for example, show no pellet-specific influence on the L → H transition power threshold P_{LH}. Obviously, as pellets do increase the plasma density, this in turn elevates P_{LH} as predicted for these plasma parameters [15]. In addition, a detailed study showed that the divertor and SOL geometry can have a strong impact on P_{LH} [21]. Comparing the pellet-fuelled discharges with the density scan performed by gas fuelling showed no difference in L → H threshold behaviour [21]. Data with pellet fuelling align well with gas-fuelled data in the same plasma configuration, and any applied combination of these two fuelling methods resulted in the same P_{LH} value for the same resulting plasma density. Hence, data taken from both the pellet-controlled case and the reference phase showing virtually identical edge profiles in order to achieve sufficient precision were considered appropriate for a plasma stability analysis.

Electron density and temperature profiles, obtained for this stability analysis are shown by the solid and dashed lines in Figure 6. A fitting procedure modelled data by a modified hyperbolic tangent function quantifying the edge barrier properties by a set of pedestal parameters. The fitting procedure considers the instrument function effect [23]. Experimental data were taken from the high-resolution Thomson scattering (HRTS) system optimized for a good resolution of the plasma edge. Several profiles covering about 200 ms, recorded at a 20 Hz framing rate, were superposed in order to allow for less uncertainty in the fit. H-mode profiles, represented by the solid lines, are selected in the pre-ELM phase, in a time interval from 70% to 99% of the ELM cycle. Profiles taken immediately after an ELM were deselected. As a cross-check, comparison with the data taken by the electron cyclotron emission (ECE) diagnostics confirmed the HRTS temperature data. Within the uncertainty of the analysis, there is no difference in the edge profiles of the reference (blue dots and solid in Figure 6) and the pellet-paced discharge (shown in red). For comparison, profiles taken during the preceding L-mode phase of the reference shot (taken at 56.8 s, fits only shown without data points) are also displayed, as dashed lines.

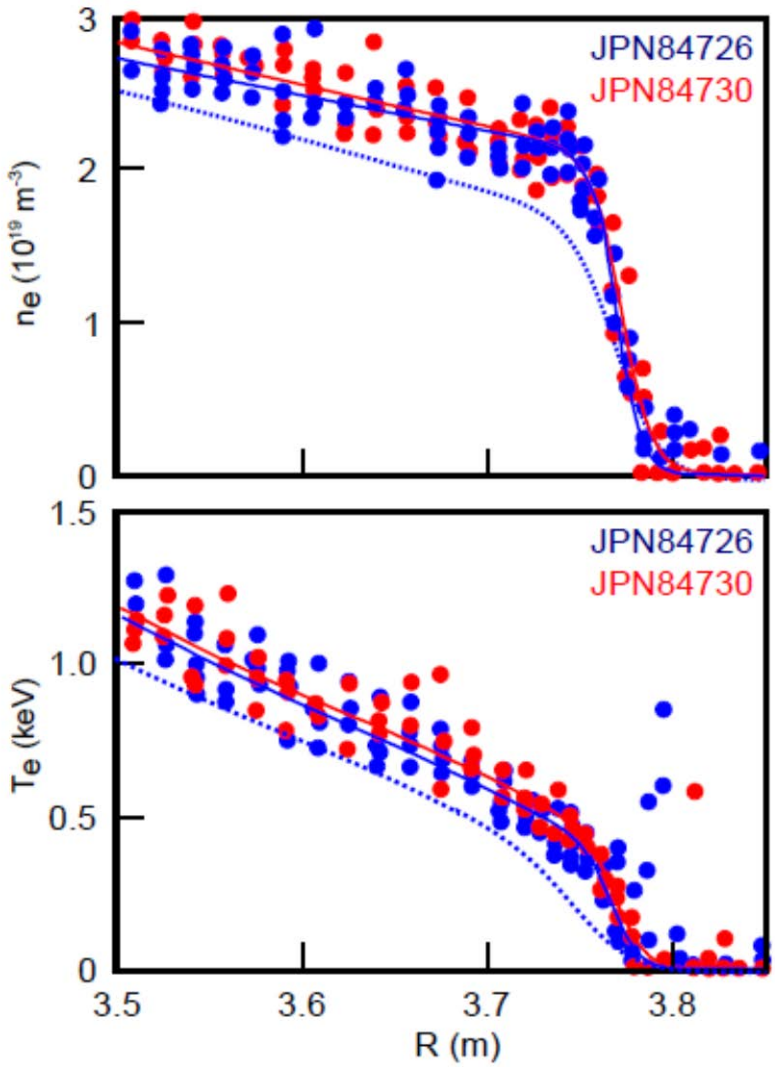

Figure 6: Edge density (upper box) and temperature profiles (lower box) from the phase following the L → H transition (dots: data points, solid lines: fits). No significant differences are found for the reference case (blue) and that with ELMs pellet-triggered early (red). Profiles from a preceding L-mode phase are displayed by the dotted lines.

The absence of ELMs for the reference case makes the amount of data and hence the fit quality somewhat higher. This represents a case where the heating power was just slowly ramped up for precise determination of P_{LH} and the pedestal just starts evolving; it was recognized as one of the lowest pressure gradients yet observed in JET H-mode plasmas. As a consequence, the plasma edge is very stable against peeling-ballooning modes.
Hence, it can be concluded that an ELM can be triggered by a strong local 3D perturbation already significantly before the pedestal has attained its linear stability limit, as predicted, for example, by the JOREK non-linear MHD code upgraded to include an appropriate description of the pellet ablation physics [24]. Simulations show that pellet triggering of ELMs can be caused by the toroidally localized high edge pressure regions produced by the localized deposition of particles by the pellet and their reheating by the plasma [25].

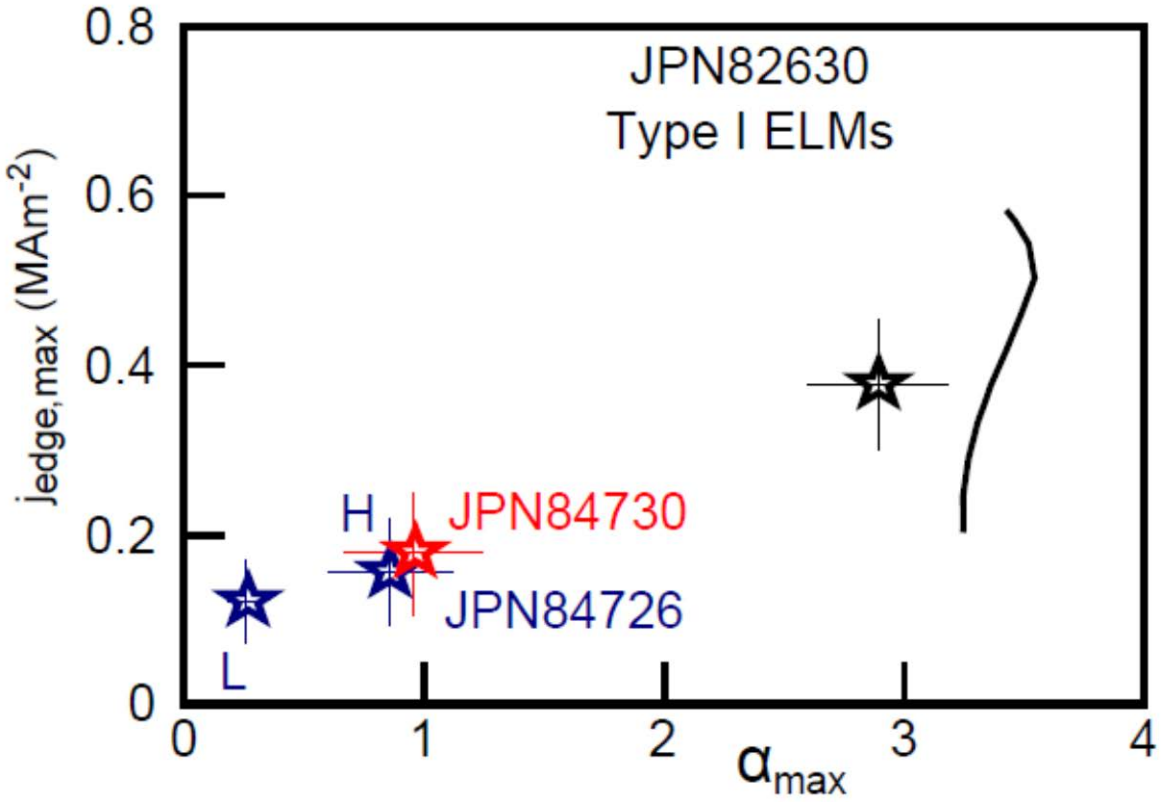

Figure 7: Edge stability diagram (maximum normalized pressure gradient α_{max} versus maximum edge current density $j_{edge,max}$, for details see [26]) of a similar comparison discharge showing type-I ELMs at an operational point (black star) close to the calculated peeling–ballooning stability (solid black line). The operational point found for pellet ELM pacing (red star) is found quite far from the stability boundary, as well the pre-ELM profiles of the reference (right blue star). The L-mode reference is displayed as well (left blue star).

For the stability analysis (for details of the method see [26]) 2D equilibria were created that matched the actual plasma as closely as possible. It is understood assuming 2D axisymmetry disregards the full 3D nature of the imposed pellet perturbation taking into account just profile modifications once the perturbation has equilibrated toroidally. A plasma equilibrium is reconstructed by using the fitted T_e and n_e profiles (assuming $T_i = T_e$) to calculate the bootstrap current self-consistently by means of the formula from [27]. With the current and pressure profiles as well as the plasma shape from EFIT reconstruction, the plasma equilibrium is calculated by means of the HELENA fixed boundary equilibrium code [28]. The equilibrium of this operational point is then used as a basis for stability analysis with the ELITE code [29]. For operational points found to be stable against peeling–ballooning modes (criterion used for an unstable mode $\gamma/\gamma_A > 0.03$, where γ is the mode growth rate and γ_A the Alfven frequency), usually the equilibrium is perturbed by varying the pressure gradient and current density in the edge region until the adjacent stability boundary is hit. However, we were not able to find any stability boundary in the vicinity of the operational point. Hence, the operational point was just put for illustration into the stability diagram of a normal type-I ELMy case taken for comparison from the stability analysis data base, this being similar with respect to the plasma configuration [30]. The stability diagram of the comparable scenario (I_P = 2.0 MA, B_t = 2.0, q_{95} = 3.2, ε = 1.68, δ_u = 0.35 and δ_l = 0.20, P_{NI} = 13 MW) together with the operational points from the pellet-paced and reference discharges is presented in

Figure 7. It is very clear that the plasma is very stable for modes usually associated with type-I ELM triggering. The local analysis of ideal n=∞ ballooning modes found the entire pedestal pressure gradient to be a factor of at least 2 below the stability limit, with no access to the 2nd stability region. Typical JET type-I ELMy pedestals are either close to the n=∞ ballooning stability limit or in the 2nd stability region [31]. The ELMs in these plasmas are very likely to be triggered by a non-ideal process such as a resistive instability or, as suggested by Futatani et al. [24], evolve from ballooning modes destabilized by the large 3D local pressure gradients of the pressure perturbation due to the pellet ablation. For comparison, the operational point of the L-mode reference is displayed as well in Figure 7.

CONCLUSION AND OUTLOOK

The study presented shows control of the ELM frequency by pellet pacing can be established while the plasma undergoes the L → H transition. Several aspects of an application during the initial operational phase of ITER were demonstrated one by one. Pellets can trigger ELMs although the edge still seems to be far from the peeling-ballooning stability boundary. Examples from AUG and JET are presented. The underlying physics raises the question of explaining on the one hand, the easiness of ELM control close to the L → H transition presented here and, on the other, the more intricate behaviour of pellet pacing in the stationary phase that was also found in both devices when changing from C to all-metal plasma-facing components [32].

At JET after installation of the ITER-like wall it was found that sometimes pellets do not trigger ELMs under ELMy H-mode conditions, where reliable triggering was found when operating with a C wall. Pacing and triggering attempts under steady-state plasma conditions revealed a trigger lag time, i.e. a distinct period of time after a previous spontaneous or triggered ELM where a pellet fails to trigger an ELM while it succeeds afterwards [22]. Investigations on this topic were repeated and refined at AUG, the presence of a trigger lag time in the all-metal wall device being confirmed. At AUG it turned out that the lag time does not significantly depend on pellet parameter size and speed, but decisively on the plasma scenario [33]. An investigation of the ELM triggering capability by pellets performed in different plasma scenarios has shown very different results. Quite a variation was observed in the response to a pellet triggering attempt; two extreme examples are displayed in Figure 8. A very high pellet ELM trigger potential is found under plasma conditions created by applying high auxiliary heating power together with nitrogen seeding [35] in order to protect the divertor by radiative cooling. A typical example is shown in the left part of Figure 8; a triggering pellet arriving just 1.9 ms after the onset of the previous spontaneous ELM, although the plasma had just started to recover from the ELM crash. In striking contrast, little trigger potential was found for the ITER base line scenario [34]. Such discharges are prone to impurity accumulation eventually finally causing fatal radiative losses due to a spontaneous ELM rate dropping too low. Several attempts to avoid this by pellet ELM pacing turned out not to be successful because pellets too often failed to trigger. Again, a typical case is presented in the right part of Figure 8; showing an ELM is not triggered by a pellet arriving 89 ms after the previous spontaneous ELM, i.e. already very late in the initial ELM cycle, and with the plasma almost fully recovered after the ELM crash.

Reported results on ELM control under conditions mimicking the first application in ITER are quite encouraging, especially owing to the fact that our findings for AUG and JET operated with all-metal walls agree so well. However, the unresolved issues of reliable pellet ELM pacing for the ITER baseline scenario in an all-metal wall tokamak remains.

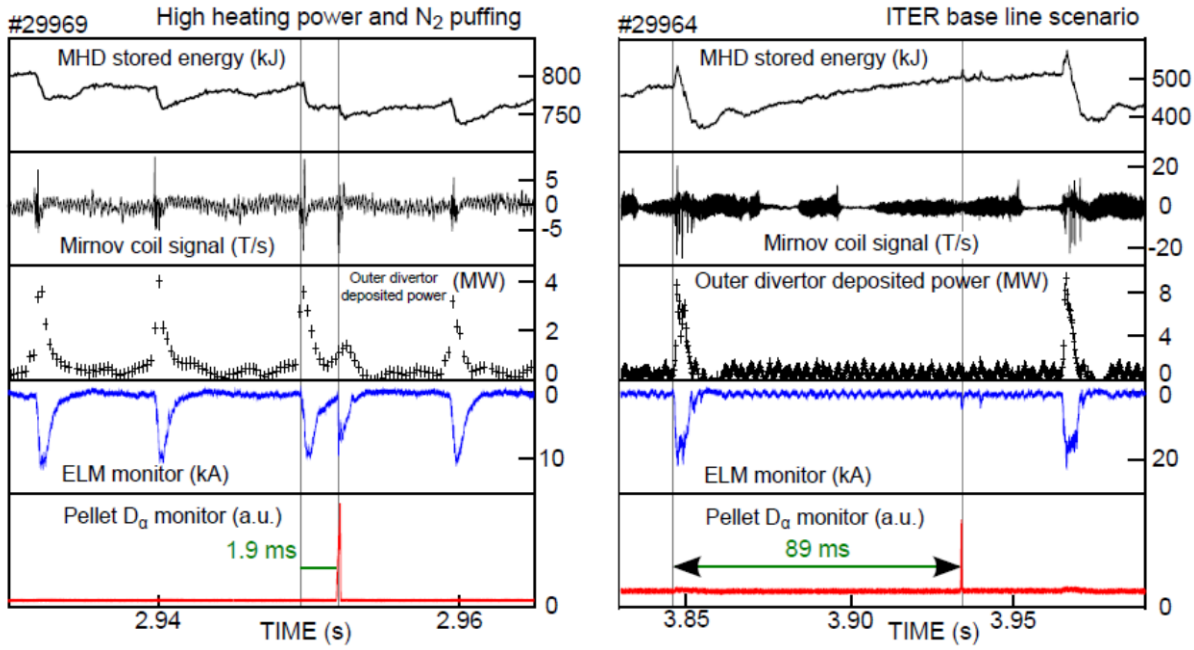

Figure 8: Most extreme cases observed for triggering lag times in AUG. Early triggering is observed in plasmas with strong auxiliary heating including nitrogen seeding for divertor cooling (left box). In the ITER baseline scenario, even a pellet arriving 89 ms after the start of the previous ELM does not succeed in triggering (right box).

Obviously, pellet ELM triggering is possible with the plasma edge far from its intrinsic stability boundary. However, severe counterexamples were observed as well. This strongly indicates that further attention must be devoted to this topic. A better understanding of the underlying physics of pellet ELM triggering is indispensable for providing reliable prediction for ITER, i.e. under what conditions pellet ELM control can be established. In particular, it would be beneficial to optimize the operational parameters of the pellet-pacing system, viz. pellet size, speed and launch position. As it is expected that pacing pellets could already carry 40% of the particle flux required for pellet particle fuelling in ITER [1], a significant reduction of this flux would ease operation by disentangling the two crucial control parameters, ELM frequency and plasma density. Furthermore, the impact of the pacing on the more crucial peak heat flux on the divertor has to be investigated. While DIII-D reports a reduction in proportion of at least the ELM frequency enhancement [6], recent investigations at AUG [33] and JET [22] found virtually no reduction. In particular, recent ELM pacing experiments at JET increasing the ELM frequency by a factor of 4 reduced the ELM-induced thermal load to the divertor by a factor of only about 1.5; for the peak heat flux virtually no reduction was found [22]. Experiments ongoing both on AUG and JET now aim to clarify the role of different plasma and pellet parameters in the triggering process. For example, the poloidal location of the pellet perturbation has shown a strong influence on the pellet trigger potential. Results from JET [36] show that inboard pellets can trigger more readily than pellets arriving at the plasma magnetic low-field side, and very recently indications of a pellet mass threshold for triggering were also found.

ACKNOWLEDGMENTS:
This work has been carried out within the framework of the EUROfusion Consortium and has received funding from the European Union's Horizon 2020 research and innovation

programme under grant agreement number 633053. The views and opinions expressed herein do not necessarily reflect those of the European Commission.

REFERENCES:

[1] A. Loarte et al., Nucl. Fusion **54** (2014) 033007
[2] G. Federici et al., Plasma Phys. Control. Fusion **45** (2003) 1523
[3] D.J. Campbell et al., in Fusion Energy 2012 (Proc.24th Int. Conf. San Diego) [ITR/P1-18] http://www-naweb.iaea.org/napc/physics/FEC/FEC2012/index.htm
[4] P.T. Lang et al., Nucl. Fusion **44** (2004) 665
[5] P.T. Lang et al., Nucl. Fusion **51** (2011) 033010
[6] L.R. Baylor et al., 2007, Nucl. Fusion **47,** 1598
[7] L.R. Baylor et al., Phys. Rev. Lett. **110** (2013) 245001
[8] S. Maruyama et al, in Fusion Energy 2012 (Proc.24th Int. Conf. San Diego) [ITR/P5-24]
[9] U. Stroth et al., 2013, Nucl. Fusion **53,** 104003
[10] B. Plöckl and P.T. Lang, Rev. Sci. Instrum. **84** (2013) 103509
[11] P.B. Parks, W.D. Sessions, and L.R. Baylor, 2000, Phys. Plasmas 7, 1968
[12] F. Romanelli and JET EFDA Contributors, 2013, Nucl. Fusion **53** 104002 http://iopscience.iop.org/0029-5515/53/10/104002/article
[13] A. Geraud et al., 27th SOFT conference, Liège (Belgium) September 2012, P1.31. http://sciconf.org/soft2012/ip/topic/c/session/p1/paper/31
[14] A, Kallenbach et al., Plasma Phys. Control. Fusion **52** (2010) 055002
[15] Y.R. Martin.et al., 2008, Journal of Physics:Conference Series **123**, 012033.
[16] F. Ryter et al., 2013, Nucl. Fusion **53,** 113003
[17] P. Gohil et al., 2001, Phys. Rev. Lett. **86**, 644
[18] M. Valovic et al., 2012, Nucl. Fusion **52,** 114022
[19] H. Zohm, Phys. Rev. Lett. **72** (1994) 222
[20] L.Schmitz et al., 2014, Nucl. Fusion **54**, 073012
[21] H. Meyer et al., Proc.41th EPS Conf. Berlin 2014, P1.013
[22] P.T. Lang et al., 2013, Nucl. Fusion **53**, 073010
[23] L. Frassinetti, 2012, Rev. Sci. Instr. **83**, 013506
[24] S. Futatani et al., 2014, Nucl. Fusion **54**, 073008.
[25] G.T.A. Huysmans et al., 2009 Plasma Phys. Control. Fusion **51**, 124012 http://iopscience.iop.org/0029-5515/53/12/123023/refs/9/article
[26] S. Saarelma et al., 2009, Plasma Phys. Control. Fusion **51**, 035001
[27] O. Sauter, C. Angioni C and Y.R. Lin-Liu, Phys. Plasmas 6, 2834 (1999).
[28] G.T.A. Huysmans, J.P. Goedbloed, W.O.K. Kerner, Computational Physics (Proc. Int. Conf. Amsterdam, 1991),World Scientific Publishing, Singapore, 371 (1991).
[29] P.B. Snyder et al., Physics. Plasmas **9**, 2037 (2002).
[30] M.N.A. Beurskens et al., 2013, Plasma Phys. Control. Fusion **55** 124043
[31] S. Saarelma et al. Nucl. Fusion **53**, 123012
[32] P.T. Lang et al., Proc.40th EPS Conf. Espoo 2013, O2.102
[33] P.T. Lang et al., 2014, Nucl. Fusion **54**, 083009
[34] J. Schweinzer et al., Proc.40th EPS Conf. Espoo 2013, P2.134
[35] A. Kallenbach et al., 2012, Nucl. Fusion **52** 122003 doi:10.1088/0029-5515/52/12/122003
[36] D. Frigione et al., Proc. 21st PSI Kanazawa 2014, P2.028